RESEARCH PAPER

Optimization of AG/RGO/TiO₂ Nanocomposite for Perovskite Solar Cells

Malik Muhammad Shahzad, Muhammad Imran*, Abdur Rafai

* Muhammad.imran@iiu.edu.pk

Department Of Mechanical Engineering, International Islamic University, Islamabad, Pakistan

Abstract: With increasing energy demand and depletion of fossil fuel resources, it is pertinent to explore renewable and eco-friendly energy resources to meet global energy demand. Recently, perovskite solar cells (PSCs) have emerged as plausible candidates in the field of photovoltaics and are considered potential contenders of silicon solar cells in the photovoltaic market owing to their superior optoelectronic properties, low cost and high absorption coefficients. Despite intensive research, PSCs still suffer from efficiency, stability, and reproducibility issues. To address the concern, the charge transport material (CTM) particularly the electron transport materials (ETM) can play a significant role in the development of efficient and stable perovskite devices. In the proposed research, we synthesized GO-Ag-TiO₂ ternary nanocomposite by facile hydrothermal approach as a potential electron transport layer (ETL) in a regular planar configuration-based PSC. The as-synthesized sample was examined for morphological, structural, and optical properties using XRD, and UV-Vis spectroscopic techniques. XRD analysis confirmed the high crystallinity of the prepared sample with no peak of impurity. The optimized GO-Ag-TiO₂ ETL exhibited a superior PCE of 8.72% with a J_{sc} of 14.98 mA.cm^{-2}, V_{oc} of 0.99 V, and a fill factor of 58.83%. Furthermore, the efficiency enhancement in comparison with the reference device is observed which confirms the potential role of doped materials in enhancing photovoltaic performance by facilitating efficient charge transport and reduced recombination. Our research suggests a facile route to synthesize a low-cost ETM beneficial for the commercialization of future perovskite devices.

Keywords: Nanocomposites, Solar Cells, Perovskite solar cells, solar cell energy optimization.

1. INTRODUCTION

Economic growth and the availability of economical renewable energy sources, like solar energy, are crucial when it comes to the global challenges of sustainable energy. Solar energy is the most durable substitute for fulfilling the world's future needs for resources that can be supplied throughout time. In photovoltaic technology [1], silicon wafers are commonly employed because of their high performance and stability (about 15% to 20%). The second generation of SCs used a-silicon or semiconductors like cadmium telluride (CdTe) and copper indium gallium selenide (CIGS) to attain a typical ten to fifteen percent efficiency level. The third generation of SCs comprises thin film photovoltaics such as DSSC, PSCs and OPVs as light harvesters. This reduced the number of raw materials needed to make the solar cells and thereby reduced production costs [2, 3].

Perovskite solar cells

A lot of research has been done on the solar cells that convert sun energy directly into electric energy are called direct solar cells. Solar cells with dye-sensitization (DSSCs) were developed by Grätzel's group. A perovskite hybrid was used to evolve them from DSSC and they harvest light [4]. When Perovskite solar cells (PSCs) made their debut, they had a low level of effectiveness [5]. Kojima et al. [6] employed $CH_3NH_3PbI_3$ and achieved low efficiency of 3.81%. These perovskite materials' variable bandgaps, high absorption coefficients, lengthy charge carrier (e$^-$ and h$^+$) diffusion lengths, and low-temperature solution processing capability are a few of its fascinating features. Figure 1 displays the rise in power conversion efficiencies (PCEs) of PSC devices over the previous few years, from 3.8 percent to 25.5 percent. Numerous initiatives and in-depth investigations into the morphological control of each functional layer, the device structural system, the regulation of perovskite crystallization, and interlayer engineering have been made [7].

A typical perovskite formula is ABX_3 derived from $BaTiO_3$, with ABX_3 being the abbreviation for ABX_3. Where X is a halogen (Cl$^-$, Br$^-$, or I$^-$) or in a mixture with other halogens as described in Eq. 1, organic cations or inorganic metal cations such as methylammonium ($CH_3NH_3^+$), formamidine ($NH_2CH=NH_2^+$), and caesium (Cs+) can be used in the A position. A quick technique

to determine whether or not certain compositions form a stable perovskite structure is to use the Goldschmidt tolerance factor (t).

$$t = (r_A + r_X) / \sqrt{2}(r_B + r_X) \tag{1}$$

Thus, as illustrated in Figure 2, rA, rB, and rX, respectively, denote the corresponding ionic radius of A, B, and X. Only when "t" is situated in the range of 0.8-1.0 can the perovskite structure be stable in three dimensions (3D) [8].
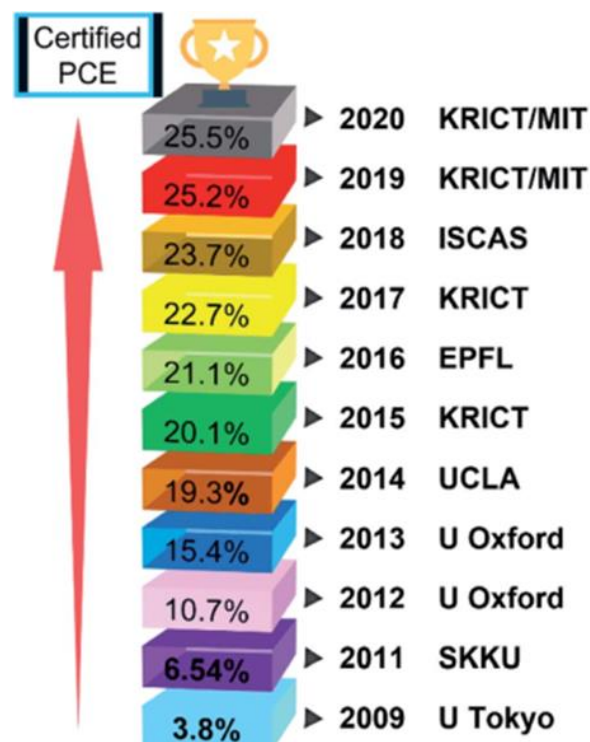
and p-i-n structures—are usually defined. Transparent conductive oxide (TCOs), is often formed on glass substrates such as FTO, ITO, and AZO. An electron transport material (ETM), a mesoporous scaffold layer, such as TiO_2, SnO_2, ZnO etc.

Fig. 1. Efficiencies of perovskite solar cells with time [5].
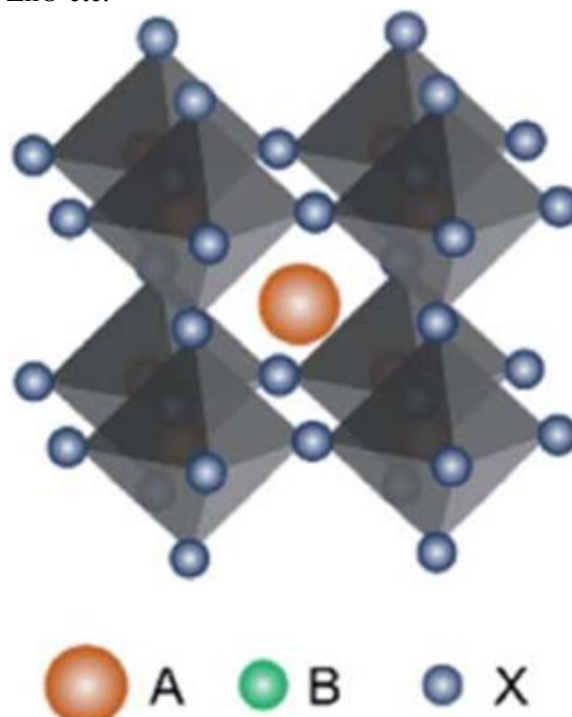

Fig. 2. Typical crystal structure of perovskite material [8].

Figure 3 illustrates a top electrode (Ag, Au), a hole transport material (HTM), and a perovskite absorption layer ($MAPbI_3$). Due to the n-i-p PSCs' planar structure without a mesoporous scaffold, the device with the mesoporous structure produces power more effectively and maintains stability over longer periods [9].
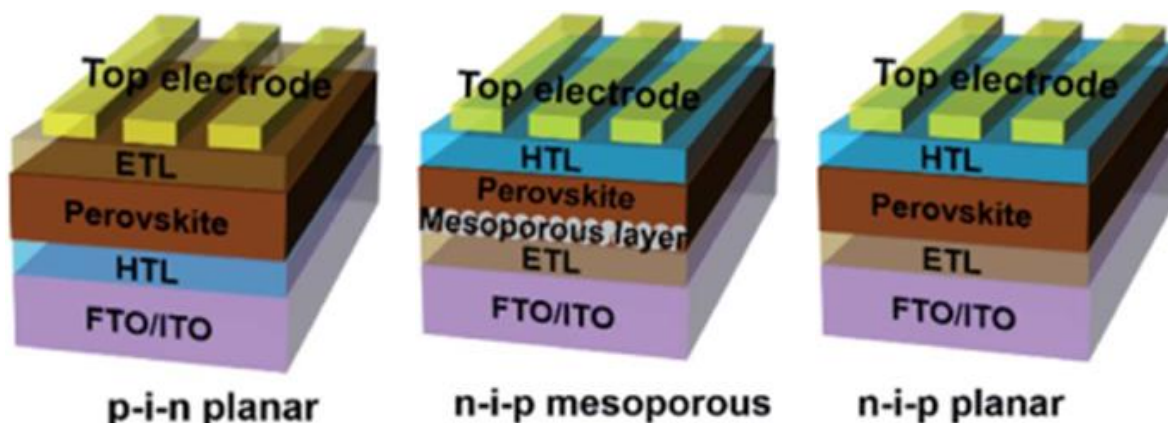
Perovskite Structures
The two types of PSC structures—n-i-p structures

Fig. 3. Planar and mesoporous structures [9]

2

Electron Transport Layer (ETL) Material

To create effective and reliable PSCs, it is necessary to follow ETL material principles including high transmittance with little optical energy loss, suitable bandgap matching, strong electrical conductivity, low cost, and good repeatability, as shown in Figure 4.

Organic ETL Material

Fullerene and its derivatives, such as PCBM or C60, are frequently utilized as ETLs in inverted PSCs owing to balanced energy level, good electron mobility, and ease of synthesis in low-temperature solution or vacuum processing. At the fullerene/electrode interface, fullerene and its derivatives, C60, bathocuproine (BCP), or bathophenanthroline (Bphen), are frequently utilized as buffer layers or interlayer to enhance the electrodes' working principles to provide a better alignment of energy levels with a lower charge extraction barrier [11].

Synthesis of TiO₂ Nanoparticles

Hydrothermal synthesis

Autoclaves with or without Teflon liners are commonly used for hydrothermal synthesis, where the reaction takes place in aqueous solutions at controlled temperatures and pressures. The pressure of vapor saturation can be accomplished by increasing the temperature above the water's boiling point. Temperature and the volume of solution added to the autoclave are the main determinants of the internal pressure of the autoclave. The hydrothermal process has also been used to make TiO_2 nanorods in addition to nanoparticles. Zhang et al. treated a $TiCl_4$ solution at 333-423 K for 12 hours to create TiO_2 nanorods.

Solvothermal Method

Solvothermal methods allow for more exact control of TiO_2 nanoparticle size, shape, and crystallinity than hydrothermal methods. Solvothermal technologies have demonstrated their adaptability to create nanoparticles with narrow size distribution and dispersion.

Fig. 4. Importance of ETL in PSCs. (a) the movement of electron e⁻ and hole h⁺ in the presence of the ETL. J-V curve comparison in a planar heterojunction arrangement (b) without and (c) with a compact ETL [10].

TiO$_2$ nanoparticles have been created using the solvothermal approach.

Fabrication of Perovskite Solar cells (PSC)

Sol-Gel Method

Numerous ceramics can be produced using the sol-gel technique. By hydrolyzing and polymerizing the antecedents, which are primarily inorganic metal or organic metal compounds like metal alkoxides, solgels are produced. Whole polymerization and solvent loss result in the conversion from a liquid sol to a solid gel. A substrate can have thin coatings applied to it using dip- or spin-coating. The wet gel that forms after the sol is poured into a mold is heated, dried, and then transformed into a thick ceramic powder. Aerogel, a very porous and extremely low-density substance, is created when the solvent from a wet gel is extracted under supercritical circumstances.

The sol-gel approach was used to produce nanostructured TiO$_2$ from titanium precursor hydrolysis. Condensation typically follows the acid-catalyzed hydrolysis of titanium (IV) alkoxide in this process. Ti-O-Ti chains are more easily formed in the reaction mixture when there is little water present, less hydrolysis occurs, and there is a lot of titanium alkoxide. Three-dimensional polymeric skeletons with tight packing have been produced as a result of the formation of Ti-O-Ti chains. Ti(OH)$_4$ formation is promoted by high hydrolysis rates and medium water content. First-order particles were freely packed due to the absence of three-dimensional polymeric skeletons and the manifestation of a significant amount of Ti-OH [12].

Oxidation Method

Titanium metal can be oxidized using oxidants or anodized to produce nanostructured TiO$_2$. A titanium metal plate has been directly oxidized with hydrogen peroxide to produce crystalline TiO$_2$ nanorods. TiO$_2$ nanorods are created when a clean Ti plate is submerged in 50 mL of a 30-weight percent H$_2$O$_2$ solution for 72 hours at 353 K. Dissolution leads to the precipitation of crystalline TiO$_2$. Inorganic salts of NaX (X= F$^-$, Cl$^-$, and SO$_4^{2-}$) can be used to change the crystalline phase of TiO$_2$ nanorods. Pure anatase can be formed with the addition of F$^-$ and SO$_4^{2-}$ while rutile can be formed with the addition of Cl. Titanium metal can also be oxidized under anodization to produce TiO$_2$ nanotubes.

For example, acetone was used to degrease a 0.05 mm thick commercially pure Ti foil, which was then rinsed with DIW and dried. Ti sample as the working electrode and the Pt plate as the CE with a 1 cm^2 anodizing exposure area. The anodizing time in solutions containing 0.5 weight percent NH$_4$F and x M malonic acid (x= 0.2) was varied from 1 second to 6 hours. An attached digital multimeter was used to record the specimen's current as it was applied with voltages ranging from 5 V to 20 V using a DC power supply. In all anodizing trials, the temperature was kept at a constant 22–2°C.

Thermal Decomposition Method

To perform thermal decompositions, Ti-based salts (TTIP or their hydrates) were first liquified in polar solvents. They were then spin-coated onto a TCO substrate, where they were gradually transformed into TiO$_2$ by thermal annealing in room-temperature air.

Steps to Improve the Capacity of TiO$_2$ ETLs

Different steps can be used to improve the abilities of TiO$_2$ ETLs in the form of charge separation, collection and efficient transfer without recombinations such as;

Doping

Elemental doping can change the electronic properties of n-type inorganic ETL materials. For PSCs, TiO$_2$ has been the preeminent ETL. Device performance has improved as a result of the addition of several elements like Li, Nb, Sn, Al, Zr, and Mg. Nb-doped TiO$_2$ is thought to boost electron injection and transport in the devices, increase the Rrec and decrease the Rs, resulting in a higher Jsc and FF. Doping TiO$_2$ with low levels of Al, Nb, and Li may help passivate the oxygen flaws and reduce surface traps [13].

Surface Modification

PSCs built from mesoporous TiO$_2$ ETLs that have undergone TiCl$_4$ treatment have shown improved solar performance. Other heterogeneous metal oxide ETLs (such as SnO$_2$), which have more negative conduction bands in comparison to TiO$_2$, exhibit the efficiency of TiCl$_4$ treatment in preventing charge recombination in a more pronounced manner.

UV-Ozone Plasma

To get rid of remaining organic species on substrates and improve the wettability of the metal oxide transport layer, UV-ozone treatment is frequently employed as a cleaning method. This would make it easier to produce perovskite films with increased surface coverage in PSCs. Additionally, it has been noted that exposure to UV-ozone may alter the electrical, and therefore photovoltaic, properties of metal oxides. Particularly, the reduction in oxygen vacancy concentration that causes a downward shift in the Fermi level could lead to an increase in the work functions of metal oxides following UV-ozone treatment.

Surface Coatings

The charge recombination at the ETL/perovskite interface is effectively suppressed by adding several wide band gap semiconductors, such as alumina, zirconia, and tungsten oxide as insulators, to the surface of n-type semiconductors.

Nano-Composite Assembly

By changing the composition of the ETL, the electrical characteristics can also be enhanced. For instance, the ETLs in PSCs have been implemented using graphene-TiO_2 nanocomposites. The high charge mobility of the graphene, which serves as an electron collector, could lower contact resistance, raise R_{rec}, and ultimately improve PCE with better Jsc, Voc, and FF. In this research study, we use silver-doped titanium dioxide (Ag-TiO_2), compared with pristine TiO_2 and their nanocomposites with reduced graphene oxide (rGO) as ETLs in conventional n-i-p planar PSCs and study their performance and stability as solar devices.

Research Gap

From the study of the above researchers, it is observed that conventional charge transport layers have been replaced by modification with noble metal nanoparticles e.g. Ag or Au. Graphene due to its fast electron mobility and large surface area has also been practically examined by constructing a TG-based ETL in PSC by various authors. It is therefore needed of the hour to examine the ternary phase comprising silver, graphene, and Titania nanoparticles. Constructing a ternary nanocomposite-based ETL can bring influential change in PSC technology due to the synergistic effect of silver and graphene.

2. EXPERIMENTAL PROCEDURES

2.1. Device Fabrication of Triple Cation Perovskite Solar Cells

The ITO substrates were cut and etched using Zinc powder and HCl followed by UV-ozone treatment. For the ETL deposition, nanocomposite dispersions in ethanol were spin-coated at 2000 rpm for 30 s followed by thermal annealing at 150°C for 60 min. For the perovskite and HTL deposition, the ETL-deposited substrates were transferred to an N2-filled glove box. The perovskite synthesis and Spiro-OMeTAD preparation are described elsewhere. The perovskite precursor was spin-coated on ITO/ETL substrates at 1000 rpm for 10 s, then 6000 rpm for 25 s. The Chlorobenzene as an anti-solvent was dropped down on the spinning substrate just before the 10 s end of the second spin-coating step. The perovskite films were then annealed at 100°C for 60 min on a hot plate. For the HTL preparation, the Spiro-OMeTAD precursors solution was spin-coated on perovskite films at 4000 rpm for 40 s. Finally, the silver contact was thermally evaporated as the back contact. The Device's active area was found to be 0.133 cm^2 measured with the help of the metal mask.

2.2. Crystalline Structural Analysis

To investigate the structural parameters, XRD is employed. The crystalline structure and phase identification are performed with the D8 Advance Bruker instrument (Germany) having the Cu Kα radiation (λ= 1.5406 Å). The step size employed was 0.02° s^{-1} with the 40 kV of accelerating voltage and the performed studies for 2θ range from 10° - 70°.

2.3. Elemental Analysis

To study the elemental composition of the samples, EDX was employed. The EDX has been used to explore the chemical composition of the ETLs, especially the nanocomposites, to study the atomic and weight percentages for the different materials with nanocomposites.

2.4. UV-Vis Spectroscopy

To study the absorbance spectra for the produced ETLs, UV-Vis spectroscopy was used. The double-beam Varian Cary 5000 instrument was

used to measure the UV-Vis absorbance spectra for the wavelength range of 300 nm – 800 nm.

2.5. Photoluminescence Studies

To study the photoluminescence effect where light energy stimulates the emission of photons from any matter. The studies were performed using a fluorescence spectrophotometer Picoquant with the laser source for the wavelength of 404 nm.

2.6. Photovoltaic Measurements

The photovoltaic measurements were performed for the Perovskite solar cells which includes the IV measurements for the devices to investigate different device parameters including the short circuit current, open circuit voltage and maximum voltages. The J-V curves were recorded under standard AM 1.5G illumination using a solar simulator attached to the Keithley 2400 source meter. Similarly, the EQE spectra were recorded using a Xenon light source attached to the KG5 filter LOT-OMENI apparatus.

3. RESULTS AND DISCUSSION

3.1. Photoluminescence Properties of ITO/ETL/Perovskite Thin Films

The steady-state photoluminescence (PL) measurements were performed to investigate the charge transport mechanism in perovskite deposited on ITO/ETL thin films. We prepared four samples in the following configuration: ITO/ TiO_2/ CsFAMA, ITO/ Ag-TiO_2/ CsFAMA, ITO/ GO-TiO_2/ CsFAMA, and ITO/ GOAgTiO$_2$/ CsFAMA and corresponding PL spectra are shown in Figure 5. The PL spectra of the Perovskite thin films exhibited a strong emission peak around 765 nm. The PL intensity was reduced for the modified ETL samples. The target sample with GOAgTiO$_2$ ETL demonstrated a less intense peak corroborating the efficient charge dissociation/extraction from perovskite to ETL. The fast charge carrier transport may be attributed to the fewer trap states in the target sample owing to GO and Ag doping [14].

The photovoltaics performance of Perovskite Solar cells using different ETLs was analyzed by measuring current-voltage (J-V) curves in Figure 6, and corresponding photovoltaics parameters listed in Table 1. The power conversion efficiency(PCE) of the target device was found

8.72% with Jsc 14.98 mA/cm^2 and Voc 0.99 V fill factor 58.83%. The substantial enhancement in photovoltaic parameters occurred due to efficient charge transport [15]. The power conversion efficiency(PCE) of the reference device was found 5.84% with Jsc 13.22 mA/cm^2 and Voc 0.9V Fill factor 49.08%. The increase in photovoltaic parameters indicates that Ag and GO doping in TiO_2 facilitated the fast charge extraction due to the good electrical conductivity of GO [16] and Ag [17]. Pristine GO doping in TiO_2 resulted in a decrease in photovoltaic parameters might be due to the irregular film formation of graphene nanosheets [18].
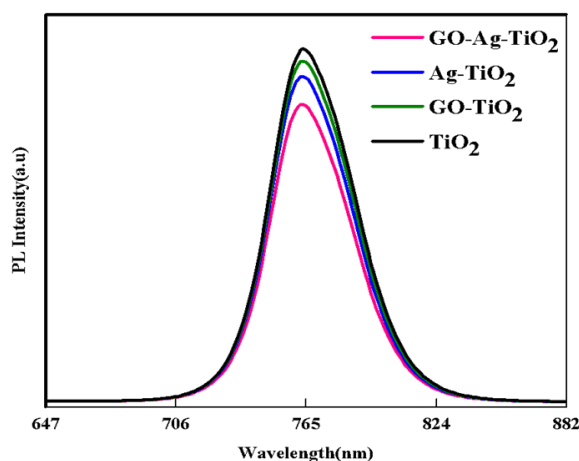

Fig. 5. Steady-state PL spectra of perovskite thin films deposited on TiO_2, Ag-TiO_2, GO-TiO_2, and GO-Ag-TiO_2 ETLs
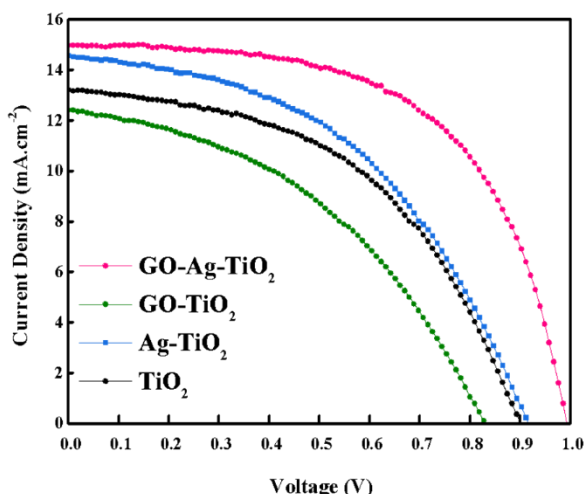

Fig. 6. J-V curves of Perovskite Solar Cells with TiO_2, Ag-TiO_2, GO-TiO_2, and GO-Ag-TiO_2 ETLs

3.2. Photovoltaic Performance of Perovskite Solar Cells Using of TiO_2, Ag-TiO_2, GO-TiO_2,

and GO-Ag-TiO₂ ETLs

Hafiz et al. [19] investigated an innovative approach involving Advanced Ag/rGO/TiO₂ ternary nanocomposites for photoanodes in highly efficient plasmonic dye-sensitized solar cells (PDSSCs). Their study showcased the successful synthesis of the Ag/rGO/TiO₂ ternary nanocomposite using a straightforward solvothermal method that avoided the use of hazardous agents. To enhance the power conversion efficiency of PDSSCs, improvements in the electron injection rate and optical absorbance of the photoanodes were deemed essential. Characterization through FE-SEM and TEM analyses confirmed the synthesis of the ternary nanocomposite. The incorporation of Ag nanoparticles onto TiO₂ nanoparticles significantly improved optical parameters through localized surface plasmon resonance (LSPR). XRD and EDX spectroscopic techniques were employed to verify the synthesis of Ag nanoparticles and rGO. Additionally, the thermal stability of the nanocomposite was assessed using thermal gravimetric analysis (TGA). The Ag/rGO/TiO₂ ternary nanocomposite-based photoanode exhibited an enhanced power conversion efficiency of 6.87% in PDSSCs, surpassing the pure TiO₂ nanoparticle-based photoanode by 15%. Moreover, a notable increase in incident photon-to-current efficiency (IPCE) of 68% was observed compared to the pure TiO₂, attributed to the exceptional conductivity of rGO. Overall, our target sample GO-Ag-TiO₂ exhibited favorable charge transport by reducing the undesirable recombination in perovskite solar cells.

The external Quantum efficiency (EQE) measurements were performed to analyze photon flux and EQE spectra are shown in Figure 7. The value of integrated short circuit current densities measured from EQE spectra was found slightly less the those obtained from JV curves the slight difference might be due to differences in the intensity of light resources [18]. The overall EQE spectra demonstrated an excellent photon flux rate over the entire visible wavelength range. Our claim is inconsistent with previous measurements.
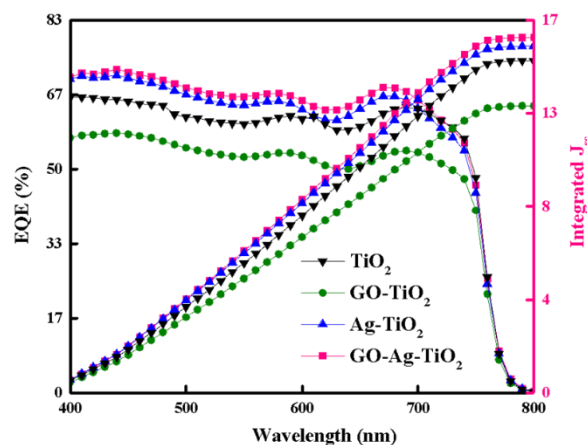

Fig. 7. EQE Spectra of Perovskite Solar Cells with TiO₂, Ag-TiO₂, GO-TiO₂, and GO-Ag-TiO₂ ETLs

4. CONCLUSIONS

In summary, we synthesized the GO-Ag-TiO₂ ternary nanocomposite by a facile hydrothermal technique to analyze the impact of silver (Ag) and graphene oxide (GO) doping on the photovoltaic performance of perovskite solar cells. The photoluminescence (PL) emission spectroscopy confirmed the efficient charge extraction by GO-Ag-TiO₂ ETL due to reduced trap states and fewer recombination centers. Further, the perovskite deposited on ITO/GO-Ag-TiO₂ ETL exhibited dense and uniform surface coverage beneficial for fast charge transport. The GO-Ag-TiO₂ ternary nanocomposite as ETL in a perovskite solar cell demonstrated a favorable PCE of 8.72% with a J_{sc} of 14.98 mA.cm^{-2}, V_{oc} of 0.99 V, and a fill factor of 58.83%. The efficiency of the modified device was found almost 33% higher than the pristine TiO2-based device. The efficiency enhancement is attributed to fast charge carrier extraction by the ETL and reduced recombinations owing to smooth and crack-free surface coverage.

Table 1. Photovoltaic Parameters of Perovskite Solar Cells with TiO₂, Ag-TiO₂, GO-TiO₂, and GO-Ag-TiO₂ ETLs

Group	ETLs	J_{SC} (mA/cm²)	V_{OC} (V)	FF (%)	PCE (%)
1	GO-Ag-TiO₂	14.98	0.99	58.83	8.72
2	Ag-TiO₂	14.57	0.92	46.83	6.28
3	TiO₂	13.22	0.90	49.08	5.84
4	GO-TiO₂	12.41	0.83	42.36	4.36

RECOMMENDATIONS FOR FUTURE WORK

The following recommendations are presented:
- The role of GO by adjusting its molar concentration should be investigated.
- Further various metal-doped GO samples can be made and tested for further devices.

CONFLICT OF INTEREST

The authors have no conflict of interest.

NOMENCLATURE/BIBLIOGRAPHY

PSC	Perovskite Solar Cells
CTL	Charge Transport Layer
CTM	Charge Transport Material
Jsc	Short Circuit Current Density
V_{OC}	Open Circuit Voltage
ETM	Electron Transport Material
ETL	Electron Transport Layer
HTL	Hole Transport Layer
HTM	Hole Transport Material
ITO	Indium Doped Tin Oxide
Ag	Silver
rGO	Reduced Graphene Oxide
TiO_2	Titanium dioxide
PCEs	Power Conversion Efficiencies
TCOs	Transparent Conductive Oxide
FTO	Fluorine doped Tin Oxide
$MAPbI_3$	Methyl Ammonia Lead Iodide
J-V	Current- Voltage
ALD	Atomic Layer Deposition
CVD	Chemical Vapor Deposition
XRD	X-ray Diffraction
SEM	Scanning Electron Microscope
EDX	Energy Dispersive X-ray Spectroscopy
UV-Vis	Ultra-Violet Visible spectroscopy
EQE	External Quantum Efficiency
PL	Photoluminescence
JCPDS	Joint Committee on Powder Diffraction Standards

REFERENCES

[1]. Gao, X. and Zhang, Y., "What is behind the globalization of technology? Exploring the interplay of multi-level drivers of international patent extension in the solar photovoltaic industry." Renewable and Sustainable Energy Reviews, 2022, 163, 112510.

[2]. Gorjian, S., Saboor, S., Ghobadian, B., Ghasemi-Varnamkhasti, M., Band, S. S., and Shokrollahzadeh, S., "Progress and challenges of crop production and electricity generation in agrivoltaic systems using semi-transparent photovoltaic technology." Renewable and Sustainable Energy Reviews, 2022, 158, 112126.

[3]. Tamin, N. N. F. and Nor, A. F. M., "Application Of Graphical User Interface in Photovoltaic Technology: A Review." Journal of Electronics, Computer Networking and Applied Mathematics (JECNAM) ISSN: 2799-1156, 2022, 2(03), 25-37.

[4]. Guo, Z., Wang, H., Liu, Y., and Zhang, M., "The high open-circuit voltage of perovskite solar cells: a review." Energy & Environmental Science, 2022.

[5]. Yu, W., Zhang, L., Li, H., Wang, H., and Chen, Z., "Recent advances on interface engineering of perovskite solar cells." Nano Research, 2022, 15(1), 85-103.

[6]. Kojima, A., Teshima, K., Shirai, Y., and Miyasaka, T., "Organometal halide perovskites as visible-light sensitizers for photovoltaic cells." Journal of the American Chemical Society, 2009, 131(17), 6050-6051.

[7]. Zhen, C., Li, Y., Yang, J., Li, X., and Sun, K., "Strategies for Modifying TiO_2 Based Electron Transport Layers to Boost Perovskite Solar Cells." ACS Sustainable Chemistry & Engineering, 2019, 7(5), 4586-4618.

[8]. Lachore, W. L., Chen, L., Wu, Y., and Wu, Z., "Recent progress in electron transport bilayer for efficient and low-cost perovskite solar cells: a review." Journal of Solid State Electrochemistry, 2021, 26(2), 295-311.

[9]. Guo, Z., Cao, Y., Gao, F., and Han, Y., "Low-temperature processed non-TiO_2 electron selective layers for perovskite solar cells." Journal of Materials Chemistry A, 2018, 6(11), 4572-4589.

[10]. Shi, Z. and Jayatissa, A. H., "Perovskites-Based Solar Cells: A Review of Recent Progress, Materials and Processing Methods." Materials (Basel), 2018, 11(5).

[11]. Liu, C., Lin, Y., He, Z., Zhang, M., and

Zhu, Z., "Ultra-thin MoOx as cathode buffer layer for the improvement of all-inorganic $CsPbIBr_2$ perovskite solar cells." Nano Energy, 2017, 41, 75-83.

[12]. Javed, S., Islam, M., and Mujahid, M., "Synthesis and characterization of TiO_2 quantum dots by sol-gel reflux condensation method." Ceramics International, 2019, 45(2), 2676-2679.

[13]. Cai, Q., Wang, H., Li, H., Wang, Y., and Zhang, Q., "Enhancing efficiency of planar structure perovskite solar cells using Sn-doped TiO_2 as electron transport layer at low temperature." Electrochimica Acta, 2018, 261, 227-235.

[14]. Devi, L. G. and Kavitha, R. J. A. S. S., "A review on plasmonic metal–TiO_2 composite for generation, trapping, storing and dynamic vectorial transfer of photogenerated electrons across the Schottky junction in a photocatalytic system." 2016, 360, 601-622.

[15]. Li, D., Zhao, X., Liu, Y., and Xu, X., "Enhanced and balanced charge transport boosting ternary solar cells over 17% efficiency." 2020, 32(34), 2002344.

[16]. Park, J.-H., Kim, J., Lee, S., Lee, J. Y., and Kim, S. O., "Chemically modified graphene oxide/ polybenzimidazo benzophenanthroline nanocomposites with improved electrical conductivity." 2012, 53(18), 3937-3945.

[17]. Xu, Z., Gao, W., Zhao, L., and Zhang, X., "Highly electrically conductive Ag-doped graphene fibers as stretchable conductors." 2013, 25(23), 3249-3253.

[18]. Zhang, B., Yang, J., Li, X., and Zhen, C., "TiO_2-intercalated graphite nanosheets increasing power conversion efficiency of MAxFA (1-x) PbI_3 perovskite solar cells." 2022, 33(1), 342-353.

[19]. Hafiz, M., Shaheer, A., Ali, Z., Khan, S., and Aslam, M., "Advanced Ag/rGO/TiO_2 ternary nanocomposite based photoanode approaches to highly-efficient plasmonic dye-sensitized solar cells." 2019, 453.